BUTTERWORTH HEINEMANN

Polymer Vol. 36 No. 14, pp. 2739–2744, 1995

0032-3861/95/$10.00+0.00

Crystallization kinetics in poly(butylene terephthalate)/copolycarbonate blend

Masami Okamoto*
Toyobo Research Center, Toyobo Co. Ltd, Katata, Ohtsu, Shiga 520-02, Japan

and Takashi Inoue
Department of Organic and Polymeric Materials, Tokyo Institute of Technology, Ookayama, Meguro-ku, Tokyo 152, Japan
(Received 17 May 1994; revised 2 November 1994)

In the practical processing conditions of poly(butylene terephthalate)/copolycarbonate (PBT/cPC) blends, crystallization starts from a partially demixed melt. To understand the crystallization mechanism in commercially important blends, we carried out time-resolved light scattering, transmission electron microscopy and small-angle X-ray scattering studies of crystallization in blends with various compositions at various crystallization temperatures. Even after crystallization, memory of demixing via the spinodal decomposition remained and crystallization seems to proceed in the PBT-rich region. PBT crystal lamellae were visualized by electron microscopy and the thickness and spacing were measured by X-ray scattering analysis. Kinetic analysis by light scattering showed a regime transition from regime II to regime I. The kinetic results were successfully interpreted by the modified Hoffman–Lauritzen theory involving a two-step diffusion mechanism characteristic of crystallization of a polymer blend, i.e. mutual diffusion for the formation of the first stem at the crystal surface and self-diffusion for the attachment of following stems in the chain.

(Keywords: polycarbonate blend; poly(butylene terephthalate); crystallization kinetics)

INTRODUCTION

As in the case of neat crystalline polymer systems, the crystallization kinetics in crystalline/amorphous polymer blends has been formulated by the Hoffman–Lauritzen theory[1] with minor modifications[2]. In the blends, the amorphous polymer should diffuse away from a crystal growth front, i.e. exclusion of the amorphous polymer should take place in an order of lamellae size, at least. This will result in complicated diffusion, so that the crystallization kinetics should differ from that of neat systems. So far, such an exclusion effect has been discussed by the modified Hoffman–Lauritzen theory involving a two-step diffusion mechanism for poly(methyl methacrylate)/poly(vinylidene fluoride) blends[3]. The kinetic discussion is on crystallization from the single-phase melt. In this paper, we deal with crystallization from a partially demixed blend.

In the previous article[4], we showed that poly(butylene terephthalate)/polycarbonate (PBT/PC) blends and poly(butylene terephthalate)/copolycarbonate (PBT/cPC) blends exhibit lower critical solution temperature (*LCST*) behaviour (*LCST* = 198°C for PBT/PC and 228°C for PBT/cPC)[4]. The results raised a complicated problem for crystallization during melt extrusion, which is important in practical terms. The problem is as follows. Cold pellets of both polymers, e.g. PBT and cPC, are fed into the extruder and are then gradually heated up. After the polymer temperature exceeds both the T_g of cPC (192°C) and the T_m of PBT (225°C), phase dissolution will start. Even after attaining the *LCST* (= 228°C), dissolution will be continued, since *LCST* can elevate under shear[5]. Under the high shear rate in the extruder, *LCST* might be elevated over the barrel temperature. Thus, mixing could be done in a wide temperature window for dissolution to obtain a homogeneous mixture. However, once the melt is extruded from the nozzle, the shear rate turns to zero and *LCST* will immediately fall to the static value (= 228°C), so that the spinodal decomposition will proceed until the system is cooled down to the static *LCST*. When the system is further cooled down below T_m, crystallization will start. Crystallization should thus be from the partially demixed system. In this paper, we investigate the crystallization kinetics of the partially demixed PBT/cPC blend by time-resolved light scattering to have a better understanding for the structure development in the practically important material. It may be interesting also as a basic subject, i.e. whether crystallization from the partially demixed system differs from that from the single-phase (non-demixed) mixture or not.

EXPERIMENTAL

PBT used in this study was a commercial product of Toyobo Co. ($M_n = 4.7 \times 10^4$; Toyobo Plastic Division). A copolycarbonate (cPC) was kindly prepared and

* To whom correspondence should be addressed

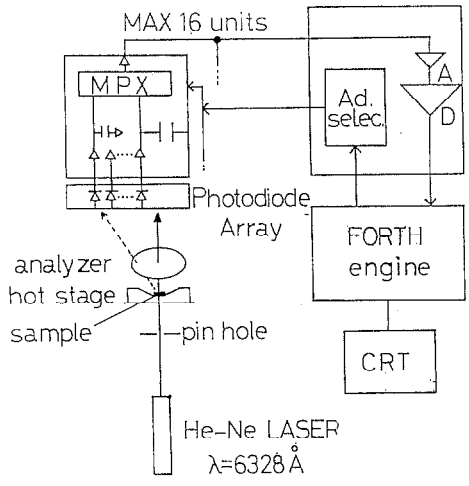

Figure 1 Light-scattering photometer equipped with 46 photodiode array for time-resolved measurement of angular dependence of scattered intensity

supplied by Mr N. Ishiai, Bayer Japan Ltd (Apec HT KU I-9360; $M_n = 2.4 \times 10^4$, $T_g = 192°C$). PBT and cPC were mixed by a co-rotating twin-screw extruder (Ikegai Machinery Corp.; 30 mm diameter, $L/D = 16$, barrel temp. = 280°C). The extruded melt was quenched in ice-water to freeze the two-phase structure in the extrudate. The quenched blend was placed between two cover glasses and melt-pressed to a thin film (ca. 20 μm thick) at 240°C ($> T_m$ of PBT and *LCST*) for 1 min†. Then the re-melt underwent a rapid temperature drop to the crystallization temperature by putting it in a hot stage set on light scattering apparatus. Immediately after the temperature drop, the time-resolved light scattering measurement was carried out as follows. In *Figure 1* is shown a light-scattering photometer. The one-dimensional photometer is equipped with 46 photodiode array (HASC Co. Ltd) and it facilitates the time-resolved measurement of scattering profile (angular dependence of scattered light intensity) with a time slice of 1/30 s[6]. One can observe the change of light scattering profile with time after the temperature drop at appropriate intervals. The radiation of a polarized He–Ne laser of 632.8 nm wavelength was applied vertically to the film specimen and the scattering profile was observed at azimuthal angle of 45° under Hv (cross-polarized) optical alignment.

Melting point was measured by a Perkin-Elmer differential scanning calorimeter, DSC-7. The heating rate was 20°C min^{-1}. The mixture was placed in an aluminium pan and it was isothermally crystallized for more than 0.5 h at various crystallization temperatures (to carry out 'Hoffman–Weeks plot').

A thick film (ca. 1 mm) for the small-angle X-ray scattering (SAXS) was also prepared by re-melt pressing and inserted into a hot stage set at the crystallization temperature under a nitrogen atmosphere. After the crystallization, the specimen was quickly quenched to liquid-nitrogen temperature to freeze-in the structure developed during crystallization. The SAXS profile of crystallized specimen was observed on a Rigaku Denki RD-RC X-ray diffraction apparatus using nickel-filtered CuK_α radiation with a wavelength $\lambda = 0.154$ nm (45 kV, 150 mA). The crystallized specimen was stained with ruthenium tetroxide and microtomed into ultrathin sections of ca. 0.1 μm thickness. The frozen morphology was observed under transmission electron microscopy (TEM), using a Hitachi H-600 (100 kV).

RESULTS AND DISCUSSION

Figure 2 shows a typical example of the morphology of the isothermally crystallized blend (PBT/cPC 50/50, at

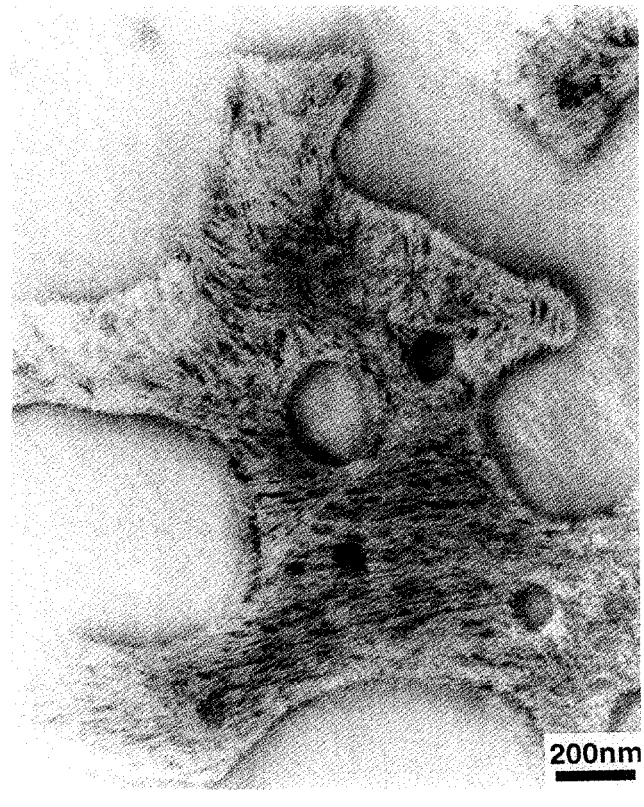

Figure 2 Transmission electron micrograph (RuO_4) of PBT/cPC 50/50 blend isothermally crystallized at 215°C for 0.5 h

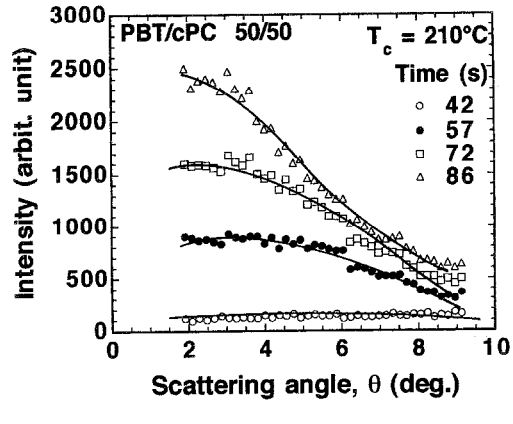

Figure 3 Change in Hv light-scattering profile at azimuthal angle 45° of PBT/cPC 50/50 blend with time after the temperature drop from 240°C to 210°C

† As mentioned above, the single-phase melt undergoes spinodal decomposition after it is extruded and the decomposed structure will be fixed by the ice-water quenching. By re-melting at 240°C ($> LCST$), the decomposition proceeds further. Thus, the partially demixed specimen was ready for the crystallization experiments

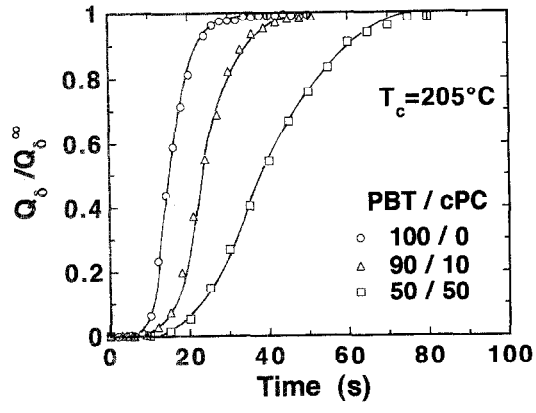

Figure 4 Time variation of light-scattering invariant Q_δ during crystallization at 205°C

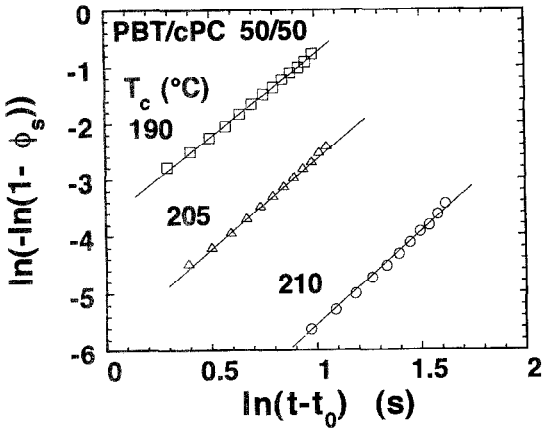

Figure 5 Avrami plots of the PBT/cPC 50/50 blend at various temperatures

215°C for 0.5 h). Both PBT and cPC phases are continuous. It suggests that the memory of spinodal decomposition before the crystallization still remains. One can also see that, in the PBT phase, the crystal lamellae appear as white stripes.

It is well known that neat PBT crystallizes to form spherulites and the four-leaf-clover type of Hv light-scattering pattern is seen for the crystallized PBT. In contrast, for the PBT/cPC blends, the four-leaf-clover character was not obvious, suggesting the formation of less ordered spherulites. This situation is demonstrated by the one-dimensional Hv scattering profiles at an azimuthal angle 45° in *Figure 3*, where the scattering maximum is not obvious even at the late stage of crystallization. Consequently, one cannot estimate precisely the average size of a spherulite by the peak angle to discuss its time variation. Anyhow, the scattering intensity increases with time of crystallization, suggesting the increase in optical anisotropy caused by the crystallization. For the kinetic discussion, instead of the scattering peak, one can employ the integrated scattering intensity, i.e. the invariant Q defined by:

$$Q = \int_0^\infty I(q) q^2 \, dq \tag{1}$$

where q is the scattering vector, $q = (4\pi/\lambda)\sin(\theta/2)$, λ and θ being the wavelength and scattering angle,

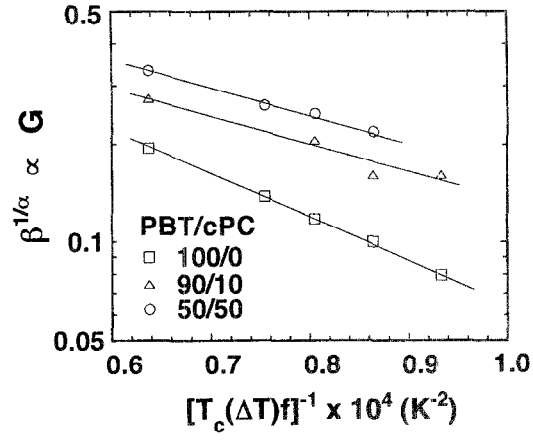

Figure 6 Temperature dependence of linear crystallization rate

respectively, and $I(q)$ is the intensity of the scattered light at q (ref. 7). The invariant in the Hv mode, Q_δ, is described by the mean-square optical anisotropy $\langle\delta^2\rangle$:

$$Q_\delta \propto \langle\delta^2\rangle \propto \phi_S(\alpha_r - \alpha_t)^2 \tag{2}$$

where ϕ_S is the volume fraction of spherulites and α_r and α_t are the radial and tangential polarizabilities of spherulites[6]. The time variation of the invariant Q_δ is shown in *Figure 4*. Q_δ^∞ is the Q_δ for very long time of crystallization ($t = 1$ h). The initial slope of Q_δ, dQ_δ/dt, is assumed to be a rate constant of crystallization. It decreases with increasing cPC content. Note that the induction time t_0 also increases with cPC content.

According to the Hoffman–Lauritzen theory on polymer crystallization[1,8], the linear growth rate of crystallite, G, is given by:

$$G \propto \beta_g \exp[-K_g/T_c(\Delta T)f] \tag{3}$$

Here β_g is a mobility term, which describes the transportation rate of crystallizable molecules to the growth front; T_c is the crystallization temperature; ΔT is the supercooling ($= T_m^\circ - T_c$, T_m° being the equilibrium melting temperature); f is the correction factor given by $2T_c/(T_m^\circ + T_c)$; and K_g is the nucleation constant, which depends on the crystallization regime (regime I, single nucleation; regimes II and III, multiple nucleation)[1,9]. The value of K_g in regimes I and III is twice that in regime II. When the Avrami equation[10] is applied for the early stage of crystallization, the time variation of ϕ_S is given by:

$$\phi_S = 1 - \exp[-\beta(t - t_0)^\alpha] \tag{4}$$

where α is the Avrami index, which depends on the mode of crystal growth or the shape of the crystallites, and β is the overall crystallization rate constant that contains nucleation. Avrami plots at the early stage for the various crystallization temperatures in the PBT/cPC 50/50 blend are shown in *Figure 5*. The plots yield straight lines, indicating that α, given by the slope, does not change with time. The constant $\alpha \approx 3$, suggesting heterogeneous nucleation and three-dimensional crystal growth. At the early stage of crystallization, the Hoffman–Lauritzen growth rate equation is given by[11]:

$$\beta^{1/\alpha} \propto \beta_g \exp[-K_g/T_c(\Delta T)f] \tag{5}$$

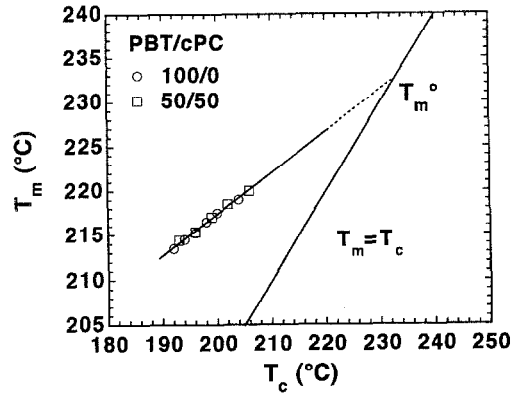

Figure 7 Hoffman–Weeks plots for neat PBT and PBT/cPC 50/50 blend crystallized isothermally at various temperatures

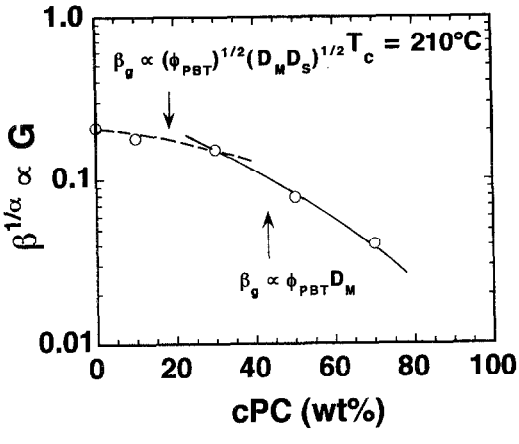

Figure 8 Linear crystallization rate *versus* cPC content at 210°C. Broken curve was calculated by equation (12) (regime II) and full curve by equation (11) (regime I); assuming $D_1^0/D_2^0 = 10$, $\gamma = 0.5$ and $n_e = 100$

Hence we can employ $\beta^{1/\alpha}$ as a growth rate G. *Figure 6* shows the value of G estimated by equation (5) as a function of $[T_c(\Delta T)f]^{-1}$. Here, the equilibrium melting temperature T_m° used is 232°C for both neat PBT and PBT/cPC blend as shown by the Hoffman–Weeks plot in *Figure 7*[12]. The $\log G$ *versus* $[T_c(\Delta T)f]^{-1}$ plot consists of a single straight line, suggesting no regime transition in the T_c window. The slope in the PBT/cPC 50/50 blend is larger than that of neat PBT (and 90/10 blend). The ratio of the two slopes is about 2. This may imply that the crystallization in 50/50 blend is classified as regime I, while in neat PBT and 90/10 blend as regime II[13].

In *Figure 8*, G is plotted as a function of composition at a fixed crystallization temperature (T_c = 210°C). The G value exhibits a weak composition dependence when cPC content is low (< 30 wt%), and a stronger dependence at higher cPC content. The results may suggest that the diffusion mechanism in the low-cPC-content blends differs from that in the higher-cPC-content blends.

Basically, the diffusion process has been described as consisting of two elementary processes: the deposition of the first stem on the growth front ('secondary nucleation process') and the attachment of following stems in the chain on the crystal surface ('surface spreading process')[1,9]. According to the Hoffman–Lauritzen theory, G is mostly governed by the rate of secondary nucleation, i, in regimes I and III, while it is governed by both i and the rate of surface spreading, g, in regime II:

$$G \propto i \qquad \text{for } i/g \ll 1 \qquad \text{(regime I)} \qquad (6)$$

$$G \propto (ig)^{1/2} \qquad \text{for } i/g \sim 1 \qquad \text{(regime II)} \qquad (7)$$

$$G \propto i \qquad \text{for } i/g \gg 1 \qquad \text{(regime III)} \qquad (8)$$

where i consists of β_g and $\exp[-K_g/T_c(\Delta T)f]$ and g consists of β_g. We define the diffusion coefficients in the surface nucleation process and the substrate completion process by D_M and D_S, respectively. Assuming that β_g is proportional to the diffusion coefficient, i and g may be given by:

$$i \propto D_M \exp[-K_g/(T_c(\Delta T)f)] \qquad (9)$$

$$g \propto D_S \qquad (10)$$

From equations (6)–(10), we obtain:

$$\beta_g \propto \phi_1 D_M \qquad \text{(regimes I and III)} \qquad (11)$$

$$\beta_g \propto \phi_1^{1/2}(D_M D_S)^{1/2} \qquad \text{(regime II)} \qquad (12)$$

where a prefactor ϕ_1 is introduced, since i is proportional to the number of crystallizable molecules at the crystal surface, which is proportional to the volume fraction of crystalline polymer ϕ_1 (ref. 2).

In the blend of crystalline and amorphous polymers, the secondary nucleation should be controlled by the two competing rate processes: the attachment of crystalline polymer onto the crystal surface and the exclusion of amorphous polymer from the surface. The competitive situation could be characterized by mutual diffusion. On the other hand, the surface spreading may be controlled by the rate of pull-out of residual segments in the crystalline chain from the melt near the growth front. It could be characterized by self-diffusion, as in the neat system. Brochard *et al.*[14] have formulated the mutual-diffusion coefficient in a binary blend of polymers 1 and 2:

$$D_M \propto \left(\frac{\phi}{D_1^0/n_1} + \frac{\phi_2}{D_2^0/n_2}\right) \qquad (13)$$

where ϕ is the volume fraction, D^0 is the diffusion coefficient of the monomer unit and n is the degree of polymerization. Equation (13) claims that the mutual diffusion is mostly governed by the slower moiety ('slow theory'). On the other hand, the self-diffusion coefficient in the blend has been formulated by Skolnick *et al.*[15]:

$$D_S \propto \frac{D_1^0}{n_1}\left(\frac{\gamma + (1-\gamma)n_1/n_2}{\gamma + (1-\gamma)n_1/n_2 + (n_1/n_e)}\right) \qquad (14)$$

where γ is a constant and n_e is the degree of polymerization between the entanglement points.

Assuming polymer 1 is PBT and polymer 2 is cPC, the ϕ_1 dependence of β_g was calculated for a particular set of values of (D_1^0/D_2^0), γ and n_e. The results are shown by the full curve (equation (11), regime I) and the broken curve (equation (12), regime II) in *Figure 8*. One sees that the open circles are nicely located on the calculated curves and the regime transition from II to I with increasing ϕ_1 is nicely interpreted. Furthermore, the calculated results for other numerical sets are shown in *Figure 9*. For all sets, the regime transition is seen. The larger the

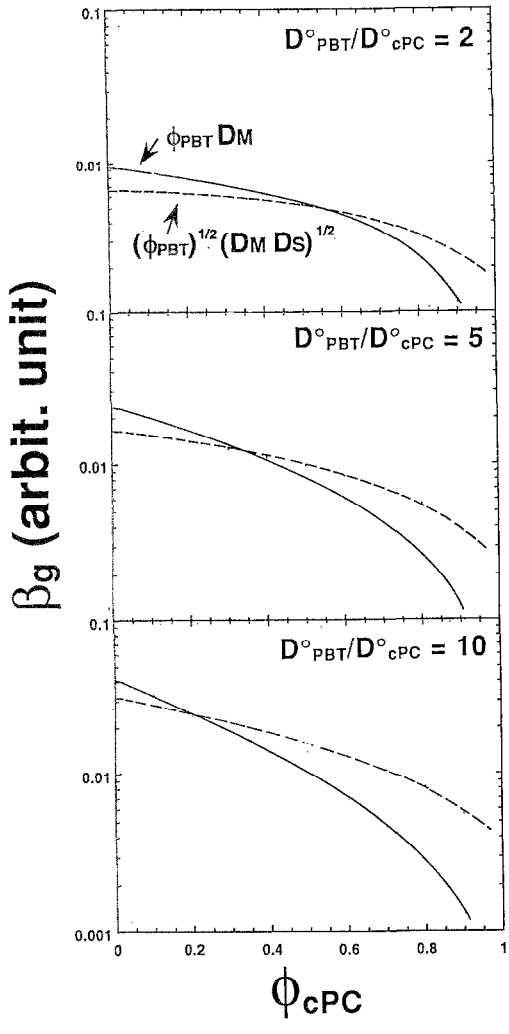

Figure 9 Calculated β_g (chain mobility term) as a function of volume fraction of cPC for various numerical settings of D_1^0/D_2^0; using equations (11) and (12)

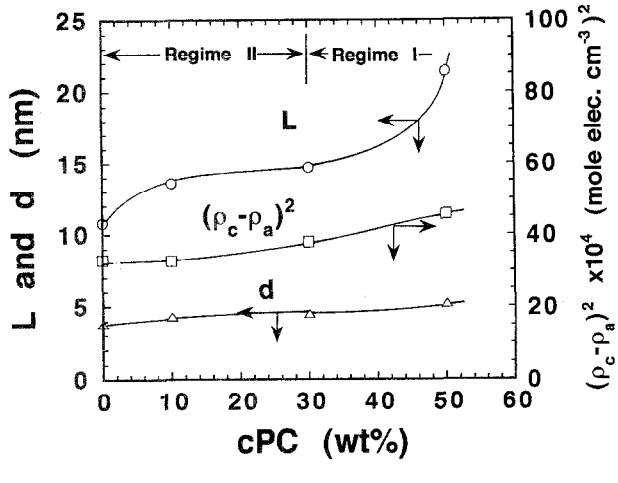

Figure 10 Characteristic parameters of crystalline morphology by small-angle X-ray scattering *versus* cPC content. Crystallization at 215°C for 0.5 h

(D^0_{PBT}/D^0_{cPC}) value, the stronger is the ϕ_1 dependence of β_g and the transition appears at smaller ϕ_1. This may suggest that the mobility of amorphous polymer strongly affects the rate of attachment of crystallizable polymer chains onto crystal surface and the incorporation of

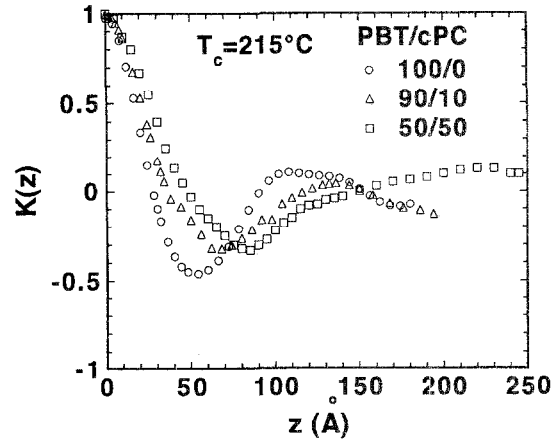

Figure 11 Linear correlation function $K(z)$ obtained by equation (15) for neat PBT, 90/10 and 50/50 PBT/cPC blends crystallized at 215°C for 0.5 h

'slow-moving impurity' provides the transition at low impurity content.

Thus, we have discussed the regime transition. One may expect that the crystallization kinetics would affect the crystalline morphology. However, no systematic results have been reported on the relationship between the morphology and the regime transition. It is one of the unsolved problems in polymer blends. Then it may be interesting to investigate the relationship for the PBT/cPC blends. The characteristic parameters for crystalline morphology determined by SAXS are plotted as a function of cPC content in *Figure 10*. The parameters were calculated by the correlation function from the desmeared data using the method of Strobl[16]. The correlation function $K(z)$ in *Figure 11* was given by[17]:

$$K(z) = \frac{\int_0^\infty s^2 j(s) \cos(2\pi z s)\, ds}{\int_0^\infty s^2 j(s)\, ds} \qquad (15)$$

where s denotes the reciprocal-space coordinate, $s = 2\sin(\theta)/\lambda$, 2θ being the scattering angle, λ is the X-ray wavelength and $j(s)$ is the scattering intensity in electron units per unit volume. We obtained the long period L, the average thickness of the crystal lamellae d and the invariant Q_{SAXS}. For an ideal two-phase system, the invariant is given by:

$$Q_{SAXS} = \phi(1-\phi)(\rho_c - \rho_a)^2 \qquad (16)$$

where ϕ is the volume fraction of crystalline phase, which is given by d/L, and $(\rho_c - \rho_a)$ is the electron-density difference between the crystal and amorphous phases. Both d and $(\rho_c - \rho_a)^2$ increase monotonically with increasing cPC content, while L hardly changes up to 30 wt% cPC content (in regime II) and starts to increase abruptly when cPC content is higher than 30 wt% (in regime I). This may imply that, by the crystallization in regime I, a larger amount of cPC is occluded between PBT lamellae, compared with that in regime II. However, at present one cannot argue why the amorphous polymer tends to remain more between crystal lamellae in regime I. Here we would like to note just the experimental results for discussion in future.

CONCLUSIONS

Thus the crystallization kinetics in the partially demixed PBT/cPC blends was nicely explained by the modified Hoffman–Lauritzen theory involving a two-step diffusion mechanism, i.e. mutual diffusion for the secondary nucleation process and self-diffusion for the surface spreading process. It suggests that there is no essential difference in the kinetics between crystallization from a single-phase (non-demixed) blend and that from a partially demixed system. The regime transition from II to I was found to take place with increasing ϕ_{cPC}.

ACKNOWLEDGEMENTS

We express our appreciation to Dr Heinz-J. Fuellmann, Bayer Japan Ltd, for fruitful discussion and we are also indebted to Mr Nobumasa Ishiai for supplying the copolycarbonate, Apec HT series.

REFERENCES

1 Lauritzen, J. I. and Hoffman, J. D. *J. Appl. Phys.* 1973, **44,** 4340
2 Boon, J. and Azcue, J. M. *J. Polym. Sci., Polym. Phys. Edn.* 1968, **6,** 885
3 Saito, H., Okada, T., Hamane, T. and Inoue, T. *Macromolecules* 1992, **24,** 4446
4 Okamoto, M. and Inoue, T. *Polymer* 1994, **35,** 257
5 Hindawi, I., Higgins, J. S. and Weiss, R. A. *Macromolecules* 1990, **23,** 670
6 Suehiro, S. and Sugimoto, K. *Nikkei Electron.* 1986, No. 396, 213
7 Koberstein, J., Russel, T. P. and Stein, R. S. *J. Polym. Sci., Polym. Phys. Edn.* 1979, **17,** 1719
8 Hoffman, J. D., Frolen, L. J., Ross, G. S. and Lauritzen, J. I., Jr *J. Res. Natl. Bur. Stand. (A)* 1975, **79,** 671
9 Hoffman, J. D. *Polymer* 1983, **24,** 3
10 Avrami, M. J. *J. Chem. Phys.* 1939, **7,** 1103
11 Lim, G. B. A. and Lloyd, D. R. *Polym. Eng. Sci.* 1993, **33,** 513
12 Martuscelli, E., Silvestre, S. and Abate, G. *Polymer* 1982, **23,** 229
13 Runt, J., Miley, D. M., Zhang, X., Gallagher, K. P., McFeaters, K. and Fishburn, J. *Macromolecules* 1992, **25,** 1929
14 Brochard, F., Jouffroy, J. and Levinson, P. *Macromolecules* 1983, **16,** 1683
15 Skolnick, J., Yaris, R. and Kolinski, A. *J. Chem. Phys.* 1988, **88,** 1407
16 Strobl, G. R. *Acta Crystallogr. (A)* 1970, **26,** 367
17 Vonk, C. G. and Kortleve, G. *Kolloid Z. Z. Polym.* 1967, **220,** 19